Theor Chem Acc (2010) 126:361–369
DOI 10.1007/s00214-009-0695-9

REGULAR ARTICLE

Theoretical design study on photophysical property of the B–N derivatives for OLED applications

Lu-Yi Zou · Zi-Long Zhang · Ai-Min Ren · Xue-Qin Ran · Ji-Kang Feng

Received: 16 July 2009 / Accepted: 4 November 2009 / Published online: 19 November 2009

Abstract The photophysical properties of a series of multifunctional compounds applied in organic light-emitting diode (OLED) materials have been studied by quantum chemistry. These compounds have been integrated by an electron and hole transporting component as well as an emitting component into the donor–π–acceptor (D–π–A) structures. To reveal the relationship between the structures and properties of these multifunctional electroluminescent materials, the ground- and excited-state geometries were optimized at the B3LYP/6-31G(d), HF/6-31G(d), and CIS/6-31G(d) levels, respectively. The ionization potentials and electron affinities were computed. The mobilities of hole and electron in these compounds were studied computationally based on the Marcus electron transfer theory. The maximum absorption and emission wavelengths of compounds **1**–**4** were calculated by time-dependent density functional theory method. As a result of these calculations, it was concluded that the electron injections of compounds **2**–**6** are much easier than Mes_2B[*p*-4,4′-biphenyl-NPh(1-naphthyl)] (BNPB) due to the introduction of the thiophene group, anthracene group, and N=N as a part of the π-conjugated bridge, compounds **5** and **6** can act as electron transport and hole transport materials, respectively. Compounds **1** and **2** have higher electron mobility and light-emitting efficiency as compared to compounds **3** and **4**. Compounds **3** and **4** have quite longer fluorescence lifetimes than compounds **1** and **2** due to the larger Stoke's shifts.

Keywords Bifunctional and multifunctional OLEDs · Optical properties · Electronic structures

L.-Y. Zou · Z.-L. Zhang · A.-M. Ren (✉) · X.-Q. Ran
State Key Laboratory of Theoretical and Computational Chemistry, Institute of Theoretical Chemistry, Jilin University, 130023 Changchun, China
e-mail: aimin.ren@gmail.com; aimin_ren@yahoo.com

J.-K. Feng
College of Chemistry, Jilin University, 130023 Changchun, China

1 Introduction

In recent publication, we reported on electronic structure and optical properties of a series of donor–π–acceptor (D–π–A) type compounds with trivalent boron as acceptor for organic light-emitting diodes (OLEDs) [1]. These D-π-A type compounds have received wide attention for the potential use in the next-generation full-color flat-panel displays since they take advantage of excellent chemical, thermal, and photochemical stabilities as well as ease of structural tuning to adjust the electronic and morphological properties [2–8]. Experimentally, amine-based π electron donors have been widely adopted in optoelectronic materials, but few reports about boron compounds with amine-based π electron donors as multifunctional OLEDs can be found due to most of the boron compounds are not stable in air [9, 10]. Thus, some bulky groups must be attached to protect the boron from attacking by oxygen. However, suitable bulky groups for protecting boron atom are very limited. Some complexes of two mesityl groups directly conjugating with boron atom are the most common and successful synthesis. Therefore, the electron transport properties of the molecules were restricted by the acceptor $B(mesityl)_2$. Nevertheless, our group's study [1] has showed that different π-conjugated bridges have greater influence on the LUMOs than HOMOs. To improve the electron transport properties, some different π-conjugated bridges are introduced into the designed molecules to

combine with B(mesityl)$_2$ in this contribution. Meanwhile, the investigation in this field has attracted great research interest and required in many applications such as in car radios, mobile phones, digital cameras, camcorders, personal digital assistants (PDAs), games, notebook personal computers (PCs), etc., due to the simplifying process and reduction of the fabrication costs of OLED devices. To our knowledge, up to now, there have been few investigation reports on bifunctional or multifunctional properties of the trivalent boron-based compounds combined with amine-group in theory and experiment. In this work, we extend our earlier theoretical study on a computational investigation of another series of amine- and trivalent boron-based bifunctional or multifunctional compounds (Fig. 1).

The dimethylamino group is chosen as the donor of the studied molecules because it is eminent donor than carbazolyl [10]. Besides the adoption of N(CH$_3$)$_2$ and B(mesityl)$_2$ as donor and acceptor, we introduced the thiophene group, anthracene group, and N=N as π-electron reservoir. It is because of that aromatic thiophene and anthracene system, and nitrogen atom could provide more rich electronic density and better electron-withdrawing ability compared to a benzene ring and carbon atom.

To rationalize the experimentally observed properties of known materials and to predict those of unknown ones, theoretical investigations on the structures, electronic spectra, and emissive properties of these materials are indispensable, especially of some parameters, such as the ionization potential (IP), electron affinity (EA), and reorganization energies (λ), which are difficult to be obtained from experiments. Thus, we apply the density functional theory (DFT), ab initio HF and configuration interaction with single excitations (CIS), and time-dependent DFT (TD-DFT) methods to investigate the geometrical structures and optical properties of these compounds such as the highest occupied orbital energies (HOMO), the lowest virtual orbital energies (LUMO), Δ_{H-L} (the energies difference between the HOMO and LUMO), the lowest excitation energies (E_g), IPs, EAs, λ, and the absorption and emission spectra are obtained and discussed in detail. The aim of the present work is to provide an in-depth understanding of optical and electronic properties of these compounds, and to offer excellent candidates for bifunctional and multifunctional OLEDs. The useful information can shed some light on designing more bifunctional and multifunctional OLED materials.

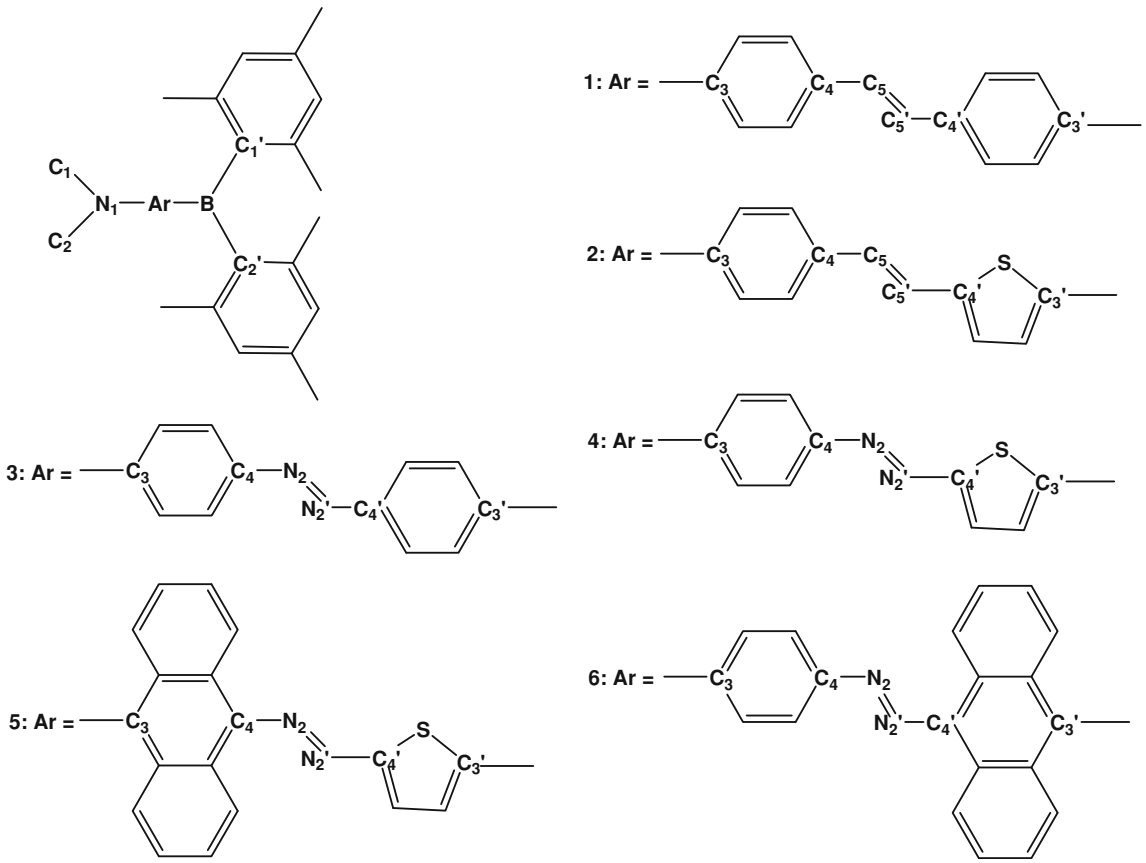

Fig. 1 Sketch map of the structures for the studied systems

2 Computation methods

All calculations of the studied compounds in this work have been performed on the SGI origin 2000 server using the Gaussian03 program package [11]. Geometric and electronic structures of the considered molecules, as well as their cationic and anionic structures, were investigated by making use of DFT. After B3LYP optimization for each ground state, the vibrational frequencies were calculated and the results showed that all optimized structures are stable geometric structures. The lowest singlet excited-state geometries were computed with ab initio CIS on the basis of the optimized geometries obtained from HF calculations. The various properties of these compounds, such as IP, EA, λ, and fluorescence lifetime (τ), were derived from the computed results. In addition, compositions of molecular orbitals and overlap populations between molecular fragments were analyzed using the PYMOLYZE program [12]. All the calculations were performed using the 6-31G(d) basis set.

3 Results and discussion

3.1 Geometry optimization

The sketch maps of the studied compounds are depicted in Fig. 1, and the optimized structures of compounds **1–6** by B3LYP/6-31G(d) are plotted in Fig. 2. The selected important bond lengths and bond angles of these compounds in the ground state, together with the available experimental values [10], are listed in Table 1. The results show that the adopted basis set and functional can reflect the change trend of the optical and electronic properties.

It can be clearly seen from Fig. 1 that compounds **1–6** have the same frame on both sides of the molecules but different π-conjugated bridges in the middle. As shown in Table 1, the substitution of anthracene for phenyl increases the bond length of N_1–C_3 in compound **5** compared with compounds **1–4** and **6**, decreases the rigidity and increases the possibility of vibration relaxation. Meanwhile, two C atoms of methyl group around N_1 atom deviate from the

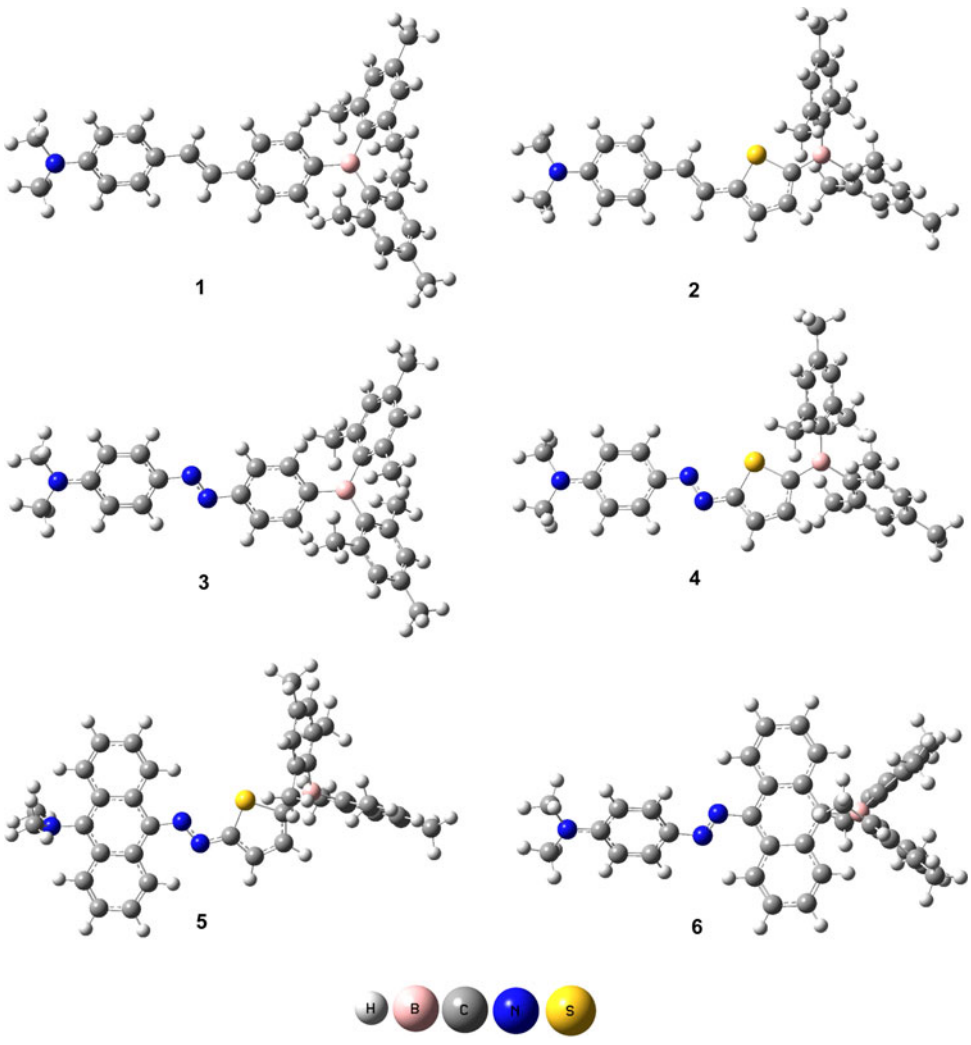

Fig. 2 The stereograph of optimized compounds **1–6** by DFT//B3LYP/6-31G(d)

Table 1 Selected important bond lengths (Å) and bond angles (°) of compounds **1–6** obtained by B3LYP/6-31G(d) calculations, as well as experimental data

	1	Exp[a]	**2**	Exp[a]	**3**	**4**	**5**	**6**
N_1–C_1	1.4528		1.4529		1.4535	1.4539	1.4560	1.4535
N_1–C_2	1.4531		1.4530		1.4538	1.4542	1.4560	1.4531
N_1–C_3	1.3852		1.3838		1.3778	1.3769	1.4320	1.3786
C_4–$C_5(N_2)$	1.4580	1.525 (8)	1.4546	1.454 (4)	1.4011	1.3950	1.3896	1.4045
$C_5(N_2)$–$C_{5'}(N_{2'})$	1.3527	1.345 (5)	1.3553	1.335 (4)	1.2678	1.2743	1.2763	1.2685
B–$C_{1'}$	1.5885	1.572 (6)	1.5887	1.571 (5)	1.5864	1.5863	1.5848	1.5864
B–$C_{2'}$	1.5879	1.566 (6)	1.5896	1.585 (4)	1.5861	1.5877	1.5862	1.5861
B–$C_{3'}$	1.5636	1.556 (6)	1.5411	1.544 (5)	1.5681	1.5485	1.5514	1.5916
$C_{4'}$–$C_{5'}(N_{2'})$	1.4606	1.554 (8)	1.4432	1.443 (4)	1.4149	1.3781	1.3753	1.4028
C_1–N_1–C_2	118.70		118.91		119.60	119.58	115.88	119.65
C_1–N_1–C_3	119.57		119.65		120.06	120.08	117.77	120.05
C_2–N_1–C_3	119.71		119.85		120.35	120.34	117.48	120.30
$C_{1'}$–B–$C_{2'}$	122.18		123.06		122.27	123.14	123.45	119.75
$C_{1'}$–B–$C_{3'}$	118.85		119.47		118.81	119.41	119.29	120.37
$C_{2'}$–B–$C_{3'}$	118.98		117.47		118.92	117.45	117.26	119.88

[a] The experimental values were subjected to X-ray diffraction study [10]

π-conjugated bridge plane in compound **5** more obvious than that in compounds **1–4** and **6.** It indicates that the anthracene group combining with N_1 atom reduced the coplanar. The lengthened N_1–C_3 bond and the reduced coplanarity in compound **5** will slow down the hole transfer rate, whereas the sums of the angles around B atom are perfectly coplanar for compounds **1–6**, irrespective of the group combining with the B atom. Furthermore, the bond of N_2=$N_{2'}$ and the heavy sulfur atom in thiophene in these compounds, strengthening the combination with the conjugated π-bridge, may enhance intersystem crossing or other non-radiation processes to quench fluorescence. However, the electron transfer rate in compound **6** will be slower than others due to the longer B–$C_{3'}$ bond length.

The CIS method has been used to obtain the excited-state geometries in this study. To compare the geometries at the same level, the ground structures of compounds **1–4** are again optimized by HF. The HF and CIS results are listed in Table 2. Interestingly, the main characters of the front orbitals, and the change trend of bond lengths and bond angles by HF are the same to that by B3LYP. The corresponding bond lengths and bond angles in each molecule have significant differences between HF and CIS methods, and imply that these complexes have large Stokes shifts. However, two carbons of methyl group around N_1 atom for compounds **1–4** in excited state is closer to be in a plane with the conjugated bridge than in their ground state, indicating that the singlet excited structures of compounds **1–4** should be more planar than in their ground structures.

3.2 Frontier molecular orbitals

It will be useful to confirm the HOMO and LUMO of molecules since the relative ordering of the occupied and virtual orbitals provides a reasonable qualitative indication of the excitation properties [13] and of the ability of electron or hole transport. Therefore, we have plotted the HOMO and LUMO of compounds **1–6** by GaussView in Fig. 3.

As shown in Fig. 3, it is noted that the electronic cloud distribution of HOMO in compounds **1–4** localizes near the nitrogen atom, while that of LUMO localizes near the boron atom. The transition from the benzene rings connected with atom N_1 to those connected with atom B is attributed to the electron push–pull effect of the substituents. The nitrogen and boron atoms are the centers of the electron donor and acceptor, respectively. Meanwhile, to observe and shed light more easily on the chemistry activity of these compounds with the same D and A, but different π-conjugated bridges in HOMO and LUMO, the local density of states (LDOS) have been compared in Table 3. From Table 3, compared with compounds **1** and **3**, the π-conjugated bridges of compounds **2** and **4** have more rich electronic density in both HOMO and LUMO due to the thiophene group. However, the electronic cloud distribution of HOMO and LUMO in compounds **5** and **6** almost localizes at the π-conjugated bridges. In addition, the introduction of the thiophene and anthracene groups as a part of the π-conjugated bridges has more rich electronic

Table 2 Optimized important bond lengths (Å) and bond angles (°) of compounds **1**–**4** with HF/6-31G(d) and CIS/6-31G(d)

	1		**2**		**3**		**4**	
	HF	CIS	HF	CIS	HF	CIS	HF	CIS
N_1–C_1	1.4466	1.4477	1.4467	1.4478	1.4468	1.4471	1.4454	1.4471
N_1–C_2	1.4469	1.4474	1.4470	1.4476	1.4474	1.4468	1.4529	1.4469
N_1–C_3	1.3894	1.3638	1.3877	1.3640	1.3824	1.3912	1.4046	1.3829
C_4–$C_5(N_2)$	1.4728	1.4083	1.4702	1.4138	1.4105	1.4011	1.4103	1.3950
$C_5(N_2)$–$C_{5'}(N_{2'})$	1.3292	1.3982	1.3302	1.3930	1.2221	1.2678	1.2234	1.2743
B–$C_{1'}$	1.6003	1.6058	1.5997	1.6045	1.5988	1.6015	1.5974	1.6016
B–$C_{2'}$	1.6002	1.6058	1.6005	1.6051	1.5988	1.6014	1.5983	1.6023
B–$C_{3'}$	1.5781	1.5565	1.5609	1.5391	1.5823	1.5741	1.5688	1.5536
$C_{4'}$–$C_{5'}(N_{2'})$	1.4755	1.4038	1.4610	1.3898	1.4202	1.4149	1.3972	1.3781
C_1–N_1–C_2	116.56	119.28	116.73	119.32	117.37	116.43	112.30	117.38
C_1–N_1–C_3	118.50	120.43	118.60	120.35	119.02	118.33	117.57	118.97
C_2–N_1–C_3	118.61	120.29	118.73	120.33	119.20	118.45	116.67	119.13
$C_{1'}$–B–$C_{2'}$	122.14	121.25	123.16	122.62	122.33	122.00	123.37	123.01
$C_{1'}$–B–$C_{3'}$	118.97	119.39	119.40	119.40	118.87	119.01	119.32	119.50
$C_{2'}$–B–$C_{3'}$	118.90	119.37	117.44	117.98	118.79	119.00	117.31	117.49

density compared to benzene ring in both HOMO and LUMO.

The HOMO and LUMO energies are experimentally estimated from an empirical formula proposed by Brédas et al. [14] based on the onset of the oxidation and reduction peaks measured by cyclic voltammetry [15]. The hole and electron injection of the materials is usually estimated by the values of HOMO and LUMO, in accord with the work function values of cathode and anode. The hole transport material (HTM) with the smaller negative value of HOMO should lose their electrons more easily, while the electron transport material (ETM) with larger negative value of LUMO should accept electrons more easily. The HOMO and LUMO energies were calculated by DFT in this study. The HOMO and LUMO energies, and energy difference Δ_{H-L}s of compounds **1**–**6** are listed in Table 4. In addition, the total density of states (DOS) of compounds **1**–**6** have been compared in Fig. 4 to more easily and vividly observe the varieties of the HOMOs, LUMOs, and energy gaps.

It can be seen from Table 4 and Fig. 4 that the HOMO and LUMO levels for compounds **1**–**4** were found to be −4.84 and −1.71, −4.81 and −1.84, −5.17 and −2.11, and −5.11 and −2.31 eV, respectively, which match well with the energy levels for Mes_2B[*p*-4,4′-biphenyl-NPh(1-naphthyl)] (BNPB) (ε_{HOMO}, −5.01 eV) and (ε_{LUMO}, −1.63 eV) [16]. Meanwhile, HOMO level of compounds **1**–**4** match well with the work function of the Indium Tin Oxides (ITO; from −4.8 to −5.1 eV) [17], and the LUMO levels are close to that of tris(8-hydroxylquinoline)aluminum (Alq_3, −1.81 eV) [18], one of the most widely used ETM. Thus, we predict that compounds **1**–**4** with similar shapes and molecular weight to BNPB may act as tri-functional (emitter, electron transport, and hole transport) molecular OLEDs. However, the introduction of the thiophene group in compounds **2** and **4** improve both of the hole and electron injection compared to compounds **1** and **3**. In addition, according to the LUMO values of these compounds, the introduction of electron-deficient N=N indeed improves the electron-injection ability compared to C=C.

Furthermore, on comparison of the results of compounds **4** with **5**, the substitution of anthracene for phenyl slightly change (0.05 eV) in HOMO, but decrease the value (0.48 eV) in LUMO. In contrary, the HOMO level in compound **6** is obviously higher (0.53 eV) than that of compound **3**, but LUMO level nearly no change (0.01 eV) due to the substitution of anthracene for phenyl. The LUMO value of compound **5** is lower 0.98 eV than that of Alq_3, showing its good ET ability. The HOMO value of compound **6** is higher than that of the well-known HTM *N*,*N*′-di-1-naphthyl-*N*,*N*′-diphenylbenzidine (NPB, −4.732 eV) [19], showing its good HT ability. According to the results of compounds **5** and **6**, it can be deduced that compounds **5** and **6** may act as ETM and HTM, respectively. In addition, the introduction of thiophene group, anthracene group, and N=N in π-conjugated bridge makes the HOMO–LUMO gaps become narrow. The order of Δ_{H-L} for compounds **1**–**4** is **1** > **3** > **2** > **4**, which determines that the absorption spectra of compounds **1**, **3**, **2** and **4** are gradual red-shifted.

3.3 IPs and EAs

The adequate and balanced transport of both injected electrons and holes are important in optimizing the

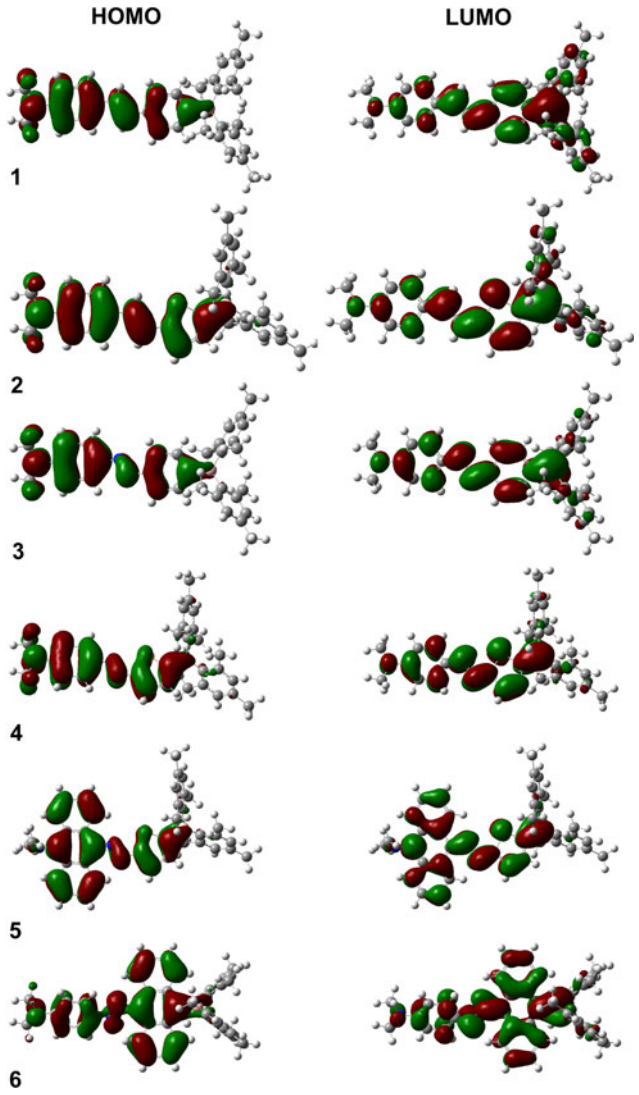

Fig. 3 Electronic density contours of the frontier orbitals for compounds **1–6**

Table 3 The contribution of electron density (%) of the donor, acceptor and π bridge to HOMO and LUMO for compounds **1–6**

	D group		π group		A group	
	HOMO	LUMO	HOMO	LUMO	HOMO	LUMO
1	35.2	0.6	63.7	41.8	1.2	57.5
2	22.5	2.1	73.0	63.9	4.5	34.1
3	29.6	3.6	67.8	74.9	2.7	21.6
4	23.8	3.8	70.6	77.7	5.6	18.5
5	1.3	1.3	94.5	88.6	4.3	10.1
6	6.8	2.9	89.3	82.6	3.9	14.5

performance of OLED devices. The IP and EA are well-defined properties that can be calculated by DFT to estimate the energy barrier for the injection of both holes and

Table 4 Negative value of the HOMO ($-\varepsilon_{HOMO}$) and LUMO ($-\varepsilon_{LUMO}$) energies, and HOMO–LUMO gaps calculated by DFT for compounds **1–6** (eV)

	1	**2**	**3**	**4**	**5**	**6**
$-\varepsilon_{HOMO}$	4.84	4.81	5.17	5.11	5.16	4.64
$-\varepsilon_{LUMO}$	1.71	1.84	2.11	2.31	2.79	2.12
Δ_{H-L}	3.13	2.97	3.06	2.80	2.37	2.52

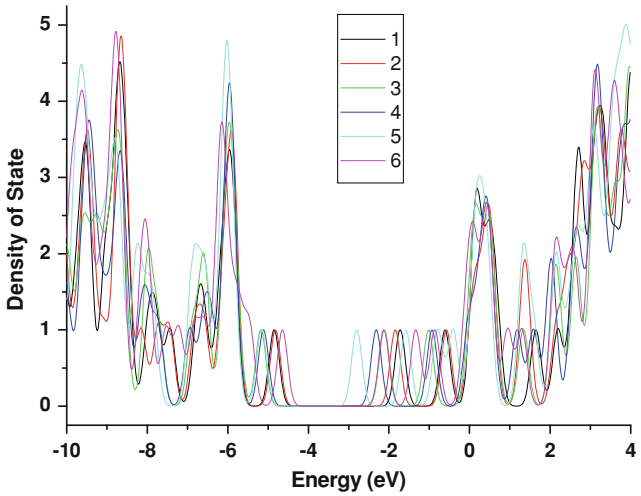

Fig. 4 Total of density of states of compounds **1–6**

Table 5 Ionization potentials, electron affinities, extraction potentials and reorganization energies for each molecule (eV)

	IP (v)	IP (a)	HEP	EA (v)	EA (a)	EEP	λ_{hole}	$\lambda_{electron}$
1	6.13	5.98	5.83	0.59	0.74	0.89	0.30	0.30
2	6.05	5.89	5.72	0.68	0.84	1.01	0.33	0.33
3	6.44	6.33	6.09	0.92	1.16	1.41	0.35	0.49
4	6.32	6.17	5.99	1.11	1.34	1.59	0.33	0.48
5	6.30	5.82	5.60	1.67	1.85	2.02	0.70	0.35
6	5.75	5.60	5.41	1.04	1.36	1.67	0.34	0.63

electrons into the compounds. Table 5 contains the calculated IPs, EAs, both vertical (v; at the geometry of the neutral molecule) and adiabatic (a; optimized structure for both the neutral and charged molecule), and the extraction potentials (HEP and EEP for the hole and electron, respectively) that refer to the geometry of the ions [20, 21].

One general challenge for the application of small molecules in OLEDs is achievement of high EA conjugated molecules for improving the electron injection/transport and low IP conjugated molecules for better hole injection/transport in electronic devices. For an electroluminescent material, the lower the IP of the hole transport layer (HTL) itself, the easier will be the injection of holes

from ITO to HTL, the higher the EA of the electron transport layer (ETL) itself, and easier the injection of electrons from cathode to ETL. Also, it has been experimentally proved that BNPB is a good trifunctional molecule [5]. From Table 5, it is can be seen that the IPs of compounds **1**–**4** are close to that of BNPB (6.09 eV), suggesting compounds **1**–**4** can be applied as the HTL materials. Remarkably, analyzing the values of EAs, compounds **2**, **3**, and **4** are easier to accept an electron than BNPB (0.74 eV) [16], despite of the same acceptor of compounds **2**, **3**, **4** and BNPB. Therefore, compounds **2**, **3** and **4** exhibit more excellent properties as electron-injection materials than BNPB due to the presence of various π-conjugated bridges. In addition, the EAs of compound **5** are significantly higher than others and BNPB, showing better ET ability. The IPs of compound **6** are obviously lower than others and BNPB, showing excellent HT ability.

At the microscopic level, the charge-transport mechanism in thin film can be described as a self-exchange transfer process, in which an electron or hole transfer occurs from one charged molecule to an adjacent neutral molecule. The rate of intermolecular charge transfer (K_{et}) can be estimated from Marcus theory [22–24] given in

$$K_{et} = A \exp\left[\frac{-\lambda}{4k_b T}\right] \quad (1)$$

where T is the temperature, A is a prefactor related to the electronic coupling between adjacent molecules, λ is the reorganization energy, and k_b is the Boltzmann constant. It will be seen that variations in the reorganization energies, which are exponential component (Eq. 1), dominate the changes in overall carrier transfer rates as the molecular structures are varied. For efficient charge transport, the reorganization energy requires to be small. At this stage, our discussion focuses on the reorganization energy.

The λ value is generally determined by fast changes in molecular geometry (the inner reorganization energy λ_i) and by slow variations in solvent polarization of the surrounding medium (the external contribution λ_e). In the case of LEDs (there are condensed-state systems), however, the latter contribution can be neglected, so that the former becomes the dominant factor. The inner reorganization energy λ_i for hole transfer can be expressed as follows:

$$\lambda_{hole} = \lambda_0 + \lambda_+ = \left(E_0^* - E_0\right) + \left(E_+^* - E_+\right) \quad (2)$$

where E_0 and E_+ represent the energies of the neutral and cation species in their lowest energy geometries, respectively, while E_0^* and E_+^*represent the energies of the neutral and cation species with the geometries of the cation and neutral species, respectively. In this way, $\lambda_{electron}$ for electron transfer can be expressed as follows:

$$\lambda_{electron} = \lambda_0 + \lambda_- = \left(E_0^* - E_0\right) + \left(E_-^* - E_-\right). \quad (3)$$

The calculated λ_{hole} and $\lambda_{electron}$ are also listed in Table 5. As materials with an emitting layer, they need to achieve the balance between hole injection and electron acceptance. The data (Table 5) show that the difference between the λ_{hole} and $\lambda_{electron}$ for compounds **1**–**4** are less than 0.15 eV, implying that they can act as the emitter with relatively high light-emitting efficiencies. However, compounds **1** and **2** have better equilibrium properties than compounds **3** and **4** due to the bond of C_5=$C_{5'}$. Replacement of N_2=$N_{2'}$ with C_5=$C_{5'}$ has no positive effect on the balance between hole transfer and electron transfer, but it improves the entrance of electrons from cathode to ETL. Furthermore, the lower the λ values, the bigger the charge-transport rate. The $\lambda_{electron}$ for compound **5** is quite smaller than its λ_{hole}. It suggests that the electron transfer rate is higher than the hole transfer rate. The case is just the contrary in compound **6** due to the quite smaller of λ_{hole} than $\lambda_{electron}$. These indicate that compounds **5** and **6** can act as ETL/a hole-block layer and HTL/an electron-block layer, respectively. The results confirm that the prediction from the geometry optimization discussion earlier. Meanwhile, the value of $\lambda_{electron}$ is increased in the order from **1** to **2** to **4** and then to **3**.

3.4 Absorption spectra and emission spectra

The transition energies, oscillator strengths, and configurations relevant to the singlet excited states in each molecule are listed in Table 6, accompanying with the

Table 6 Absorption spectra obtained by TD-DFT method for compounds **1**–**4** at the B3LYP/6-31G(d) optimized geometries

	Electronic state change	λ_{max}^{abs} (nm)	Exp[a] (nm)	f	Excitation energies (eV)	Main configurations and coefficient	
1	$S_0 \rightarrow S_1$	430.8	403	1.13	2.88	HOMO → LUMO	0.66
2	$S_0 \rightarrow S_1$	452.2	431	1.14	2.74	HOMO → LUMO	0.64
3	$S_0 \rightarrow S_2$	434.1		1.25	2.86	HOMO → LUMO	0.63
4	$S_0 \rightarrow S_2$	471.1		1.19	2.63	HOMO → LUMO	0.61
						HOMO-4 → LUMO	0.10

[a] Measured in THF

experimental results. As shown in Table 6, all the electronic transitions are $\pi \rightarrow \pi^*$ type. Due to the different double bond in the central position of the π-conjugated bridge, the strongest absorption peaks with largest oscillator strength for compounds **1** and **2**, and **3** and **4** are assigned to the electronic state change of $S_0 \rightarrow S_1$, and $S_0 \rightarrow S_2$, respectively. The electronic excited states S_1 and S_2 are mainly dominated by the transition HOMO $\rightarrow$ LUMO. The λ_{max}^{abs} for compounds **1**, **3**, **2** and **4** is red-shifted, $430.8 < 434.1 < 452.2 < 471.1$ nm (Fitted Gaussian type absorption curves with the calculated absorption data are shown in Fig. 5), which is in accord with the decrease in the HOMO–LUMO gaps.

As shown in Table 7, it can be seen that the emission peaks with the large oscillator strength are all assigned to $\pi \rightarrow \pi^*$ character arising from S_1, HOMO $\rightarrow$ LUMO transition. The calculated values of the fluorescence wavelength for compounds **1–4** are located at 457.1, 482.8, 511.7, and 519.1 nm, respectively. However, two factors may cause deviations of our calculated data from the experiment values. One is that the calculation of these compounds was on the basis of isolated gas-phase, and the experiment values were measured in the liquid phase involving the environmental influences. Another factor that should be born in mind is that polarization effects and intermolecular packing forces had been neglected in the calculations. From the oscillator strength, and coefficient and configurations, the introduction of N=N in compounds **3** and **4** indeed reduced fluorescence compared to compounds **1** and **2**.

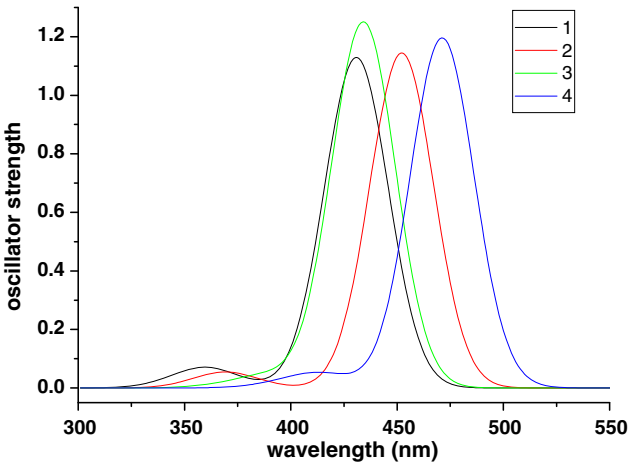

Fig. 5 Simulated absorption spectra of compounds **1–4** with the calculated data at the TDDFT/B3LYP/6-31G(d) level

Based on the calculated emission spectra from 457.1 to 519.1 nm, we predict that compounds **1–4** could be used as blue and green light-emitting materials. Meanwhile, the Stoke's shifts of these compounds are within the range from 26.3 to 77.6 nm. It may be explained that these compounds have large change of the structures in the ground and excited states. Furthermore, the radiative lifetimes have been computed for spontaneous emission using the Einstein transition probabilities according to the formula (in au) [25, 26]:

$$\tau = \frac{c^3}{2(E_{Flu})^2 f}$$

where c is the velocity of light, E_{Flu} the excitation energy, and f is the oscillator strength (see Table 7). The computed lifetime τ for compounds **1**, **2, 3**, and **4** are $\sim$1.99, 2.55, 45.06, and 12.66 ns, respectively, the order of τ are **1** > **2** > **4** > **3**. The sequence of fluorescence lifetimes is in accordance with the sequence of the Stoke's shifts.

4 Conclusions

In this study, the ground-state and excited-state properties of these compounds were investigated by DFT, HF, TDDFT, and CIS methods. From the above research we conclude that compounds **1–4** are ideal for applications as multifunctional OLED materials. The calculated values of IP and EA show that compounds **1–4** can be used as ETM and HTM simultaneously. Analyzing values of λ, compounds **1** and **2** have higher intra- and intermolecular charge-transfer ability and better equilibrium properties

Table 7 Emission spectra obtained by TD-DFT method for compounds **1–4** at the CIS/6-31G(d) optimized geometries

	Electronic state change	λ_{em} (nm)	Exp[a] (nm)	f	τ (ns)	Excitation energies (eV)	Main configurations and coefficient	
1	$S_1 \rightarrow S_0$	457.1	538	1.58	1.99	2.71	HOMO $\rightarrow$ LUMO	0.62
2	$S_1 \rightarrow S_0$	482.8	558	1.38	2.55	2.57	HOMO $\rightarrow$ LUMO	0.61
3	$S_1 \rightarrow S_0$	511.7		0.09	45.06	2.42	HOMO $\rightarrow$ LUMO	0.33
							HOMO-1 $\rightarrow$ LUMO	0.52
4	$S_1 \rightarrow S_0$	519.1		0.32	12.66	2.39	HOMO $\rightarrow$ LUMO	0.49
							HOMO-5 $\rightarrow$ LUMO	0.39

[a] Measured in THF

compared to compounds **3** and **4**, compounds **5** and **6** can be used as ETM and HTM, respectively. The anthracene group in different position of the π-conjugated bridge can act as bifunctional properties materials. Replacing the C=C with N=N in compounds **3** and **4** has no positive effect on charge-transport rate, but enhances the ability of the electron injection. To introduce the thiophene group, anthracene group, and N=N, the HOMO–LUMO gaps become narrow. With the HOMO–LUMO gaps decreasing, the absorption wavelengths for compounds **1**, **3**, **2**, and **4** exhibit gradual red-shifts. Meanwhile the Stoke's shifts of compounds **1**–**4** ranging from 26.3 to 77.6 nm occur due to the large change of the structures in the ground and excited states. The emission wavelengths of compounds **1**–**4** are located at blue and green range, implying that they can be used as blue and green light-emitting materials. Also, the radiative lifetimes have been computed out, which are in accordance with the order of the Stoke's shifts: $\mathbf{1} > \mathbf{2} > \mathbf{4} > \mathbf{3}$.

Acknowledgments This work is supported by the Major State Basis Research Development Program (No. 2002CB 613406) and the National Natural Science Foundation of China (No. 20673045).

References

1. Zou LY, Ren AM, Feng JK, Liu YL, Ran XQ, Sun CC (2008) J Phys Chem A 112:12172–12178
2. Li X, Wang X, Gao J, Yu X, Wang H (2006) Chem Phys 326:390–394
3. Sun Y, Wang S (2009) Inorg Chem 48:3755–3767
4. Cui Y, Li F, Lu ZH, Wang S (2007) Dalton Trans 2634–2643
5. Jia WL, Feng XD, Bai DR, Lu ZH, Wang S, Vamvounis G (2005) Chem Mater 17:164–179
6. Jia WL, Moran MJ, Yuan YY, Lu ZH, Wang S (2005) J Mater Chem 15:3326–3333
7. Bai DR, Liu XY, Wang S (2007) Chem Eur J 13:5713–5723
8. Liu XY, Bai DR, Wang S (2006) Angew Chem Int Ed 45:5475–5478
9. Liu ZQ, Cao DX, Fang Q, Liu GQ, Xu GB (2004) Acta Chim Sinica 62:2103–2108
10. Liu ZQ, Fang Q, Wang D, Cao DX, Xue G, Yu WT, Lei H (2003) Chem Eur J 9:5074–5084
11. Frisch MJ, Trucks GW, Schlegel HB, Scuseria GE, Robb MA, Cheeseman JR, Montgomery JA Jr, Vreven T, Kudin KN, Burant JC, Millam JM, Iyengar SS, Tomasi J, Barone V, Mennucci B, Cossi M, Scalmani G, Rega N, Petersson GA, Nakatsuji H, Hada M, Ehara M, Toyota K, Fukuda R, Hasegawa J, Ishida M, Nakajima T, Honda Y, Kitao O, Nakai H, Klene M, Li X, Knox JE, Hratchian HP, Cross JB, Bakken V, Adamo C, Jaramillo J, Gomperts R, Stratmann RE, Yazyev O, Austin AJ, Cammi R, Pomelli C, Ochterski JW, Ayala PY, Morokuma K, Voth GA, Salvador P, Dannenberg JJ, Zakrzewski VG, Dapprich S, Daniels AD, Strain MC, Farkas O, Malick DK, Rabuck AD, Raghavachari K, Foresman JB, Ortiz JV, Cui Q, Baboul AG, Clifford S, Cioslowski J, Stefanov BB, Liu G, Liashenko A, Piskorz P, Komaromi I, Martin RL, Fox DJ, Keith T, Al-Laham MA, Peng CY, Nanayakkara A, Challacombe M, Gill PMW, Johnson B, Chen W, Wong MW, Gonzalez C, Pople JA (2004) Gaussian 03, revision C.02. Gaussian Inc, Wallingford
12. Tenderholt A (2005) PyMOlyze, 2.0, Stanford University, Stanford, CA-94305
13. De Oliveira MA, Duarte HA, Pernaut JM, De Almeida WB (2000) J Phys Chem A 104:8256–8262
14. Brédas JL, Silbey R, Boudreaux DS, Chance RR (1983) J Am Chem Soc 105:6555–6559
15. Morisaki Y, Ishida T, Chujo Y (2003) Polym J 35:501
16. Zou LY, Ren AM, Feng JK, Ran XQ (2009) J Phys Org Chem. doi:10.1002/poc.1565
17. Huang CH, Li FY, Huang W (2005) The introduction for the organic light emitting materials and devices. Fudan University, Shanghai
18. Liu XD, Ren AM, Feng JK, Yang L, Xu H, Shi MM, Sun CC (2006) Chem J Chinese U 11:2156–2159
19. Lin BC, Cheng CP, Michael Lao ZP (2003) J Phys Chem A 107:5241–5251
20. Curioni A, Boero M, Andreoni W (1998) Chem Phys Lett 294:263–271
21. Wang I, Botzung-Appert E, Stéphan O, Ibanez A, Baldeck PL (2002) J Opt A Pure Appl Opt 4:S258–S260
22. Marcus RA (1956) J Chem Phys 24:966–978
23. Marcus RA (1993) Rev Mod Phys 65:599
24. Liao Y, Yang G, Feng J, Shi L, Yang S, Yang L, Ren A (2006) J Phys Chem A 110:13036
25. Litani-Barzilai I, Bulatov V, Gridin VV, Schechter I (2004) Anal Chim Acta 501:151–156
26. Lukeš V, Aquino A, Lischka H (2005) J Phys Chem A 109:10232–10238